HHS Public Access

Author manuscript

Mol Cancer Ther. Author manuscript; available in PMC 2021 April 01.

Published in final edited form as:

Mol Cancer Ther. 2020 October ; 19(10): 2012–2022. doi:10.1158/1535-7163.MCT-19-1116.

Polyamine Blocking Therapy Decreases Survival of Tumor-Infiltrating Immunosuppressive Myeloid Cells and Enhances the Anti-Tumor Efficacy of PD-1 Blockade

Eric T. Alexander[1], **Kelsey Mariner**[1], **Julia Donnelly**[1], **Otto Phanstiel IV**[2], **Susan K. Gilmour**[1,3]

[1]Lankenau Institute for Medical Research, 100 Lancaster Avenue, Wynnewood, PA 19096

[2]University of Central Florida, Department of Medical Education, College of Medicine, Orlando, Florida 32826

Abstract

Despite unprecedented advances in the treatment of cancer through the use of immune checkpoint blockade, responses are not universal and alternative strategies are needed to enhance responses to ICB. We have shown previously that a novel polyamine blocking therapy (PBT), consisting of co-treatment with α-difluoromethylornithine (DFMO) to block polyamine biosynthesis and a Trimer polyamine transport inhibitor, decreases myeloid-derived suppressor cells (MDSC) and M2-like tumor-associated macrophages (TAM). Both MDSCs and TAMs promote tumor progression, inhibit anti-tumor immunity, and limit the efficacy of ICB. In this study we investigated the use of PBT to heighten therapeutic responses to PD-1 blockade in mice bearing 4T1 mammary carcinoma and B16F10 melanoma tumors. Whereas PBT inhibited primary tumor growth in both tumor models, 4T1 lung metastases were also dramatically decreased in mice treated with PBT. Reductions in MDSC and TAM subpopulations in 4T1 tumors from PBT-treated mice were accompanied by reduced cytoprotective autophagy only in tumor-infiltrating MDSC and macrophage subpopulations but not in the lung or spleen. PBT treatment blunted M2-like alternative activation of bone marrow-derived macrophages and reduced STAT3 activation in MDSC cultures while increasing the differentiation of $CD80^+$, $CD11c^+$ macrophages. PBT significantly enhanced the anti-tumor efficacy of PD-1 blockade in both 4T1 and B16F10 tumors resistant to anti-PD-1 monotherapy, increasing tumor-specific cytotoxic T-cells and survival of tumor-bearing animals beyond that with PBT or PD-1 blockade alone. Our results suggest that co-treatment with DFMO and the Trimer polyamine transport inhibitor may improve the therapeutic efficacy of immunotherapies in cancer patients with resistant tumors.

Keywords

polyamines; difluoromethylornithine; transport inhibitor; immune checkpoint blockade; immunosuppression

[3]To whom requests for reprints should be addressed, at Lankenau Institute for Medical Research, 100 Lancaster Avenue, Wynnewood, PA 19096 USA; Telephone: (484) 476-8429; Fax: (484) 476-2205; gilmours@mlhs.org.

The authors declare no potential conflicts of interest.

Introduction

New cancer therapy strategies including immune checkpoint inhibitors have led to dramatic tumor regressions in some patients with metastatic cancers. Unfortunately clinical trials have revealed that use of immune checkpoint blockade (ICB) monotherapy targeting programmed cell death protein-1 (PD-1) or programmed cell death ligand-1 (PD-L1) alone is ineffective in the majority of patients with metastatic cancers [1, 2]. Because tumors employ a variety of mechanisms to facilitate immune escape, it has become clear that we must also target key survival pathways that allow tumor cells to survive cancer immunotherapy.

Polyamines are essential for survival of many tumors. Polyamines (putrescine, spermidine, and spermine) are amino acid-derived polycations that play key roles in cellular proliferation, gene expression, and autophagic states that all contribute to tumor progression [3, 4]. Polyamine levels are dramatically elevated in tumor cells compared to normal cells [3]. Oncogenes such as MYC, RAS, and $BRAF^{V600E}$ upregulate polyamine biosynthesis and increase cellular uptake of polyamines by inducing the polyamine transport system (PTS) [5–8]. Thus, tumors have a greatly increased metabolic need for polyamines compared to normal cells. Accumulating studies show that the greatly increased levels of polyamines in tumors also contribute to the immunosuppressive nature inherent in most malignant tumors [4, 9].

To starve tumors of polyamines that are essential for their growth and survival, we have developed a polyamine-blocking therapy (PBT) that includes *a combination of* 1) α-difluoromethylornithine (DFMO), an FDA-approved drug that specifically inhibits ornithine decarboxylase (ODC), a rate-limiting enzyme in polyamine biosynthesis [3, 4] and 2) a novel polyamine transport inhibitor (PTI), i.e., a three-armed-polyamine compound (Trimer PTI) [9, 10]. Normal cells are significantly less sensitive to the Trimer PTI since they have low PTS activity. We have shown that Trimer PTI accumulates in tumor tissue of tumor-bearing mice due to elevated PTS activity in tumor cells compared to normal cells [9]. In addition to depriving polyamine-addicted tumor cells of polyamines, PBT also reduces polyamine-mediated immunosuppression in the tumor microenvironment, leading to the activation of tumoricidal T-cells. Previous studies have demonstrated that the anti-tumor effect of PBT in a variety of animal tumor models is T-cell dependent and is accompanied by an increase in tumor-specific $CD8^+$ T-cells and a decrease in myeloid immunosuppressive tumor-infiltrating cells including myeloid derived suppressor cells (MDSCs) and tumor associated macrophages (TAMs) [9].

Perturbations of polyamine metabolism can impact arginine metabolism within the tumor microenvironment particularly because polyamine biosynthesis depends on arginase that supplies ornithine to ODC. The extent to which arginine is metabolized by nitric oxide synthase (NOS) or arginase is an important factor in determining the inflammatory response of macrophages and dendritic cells. Although macrophages are often described as having a proinflammatory, M1 polarized phenotype or as alternatively activated, M2 polarized macrophages that are pro-tumorigenic, TAMs *in vivo* display a continuum of phenotypes between these two extremes. However, immunosuppressive tumor-infiltrating immune cells, including MDSCs, granulocytes, immature dendritic cells, and Tregs, are all characterized

by elevated levels of arginase whose depletion of arginine severely suppresses T cell functions [11, 12]. In addition, accumulating studies indicate that polyamine synthesis may also regulate the formation of pro-inflammatory M1-like or pro-tumorigenic M2-like macrophages [13–15]. Zhang et al.[14] reported that spermine inhibits proinflammatory cytokine production in monocytes/macrophages. In another study using thioglycolate-elicited murine peritoneal macrophages, arginase-independent polyamine production stimulated the expression of M2 macrophage markers and inhibited lipopolysaccharide (LPS)-induced expression of inflammatory genes [13]. A recent study demonstrated that the myeloid-specific deletion of *ODC* in $Odc^{\Delta Mye}$ transgenic mice increases the production of proinflammatory cytokines of macrophages in response to M1 stimuli such as *Helicobacter pylori* and LPS [16, 17].

In this study, we explore the effect of lowering polyamine levels with PBT on the polarization phenotype and survival of tumor-infiltrating macrophage and MDSC populations in animal models of metastatic breast cancer and melanoma. Because PBT acts to relieve polyamine-mediated immunosuppression in tumors, we also sought to apply this polyamine targeted therapy to heighten therapeutic responses to PD-1 immune checkpoint blockade currently used clinically.

Materials and Methods

Key Resources

Detailed identification, and ordering information when applicable, of all mouse models, cell lines and antibodies used is included in Supplemental Table I.

Animals

Female C57Bl/6 and Balb/C mice were obtained from Charles Rivers/NCI. $Odc^{\Delta Mye}$ mice [16] were kindly provided by Dr. Keith Wilson of Vanderbilt University. Protocols for the use of animals in these studies were reviewed and approved by the Institutional Animal Care and Use Committee of the Lankenau Institute for Medical Research in accordance with the current US Department of Agriculture, Department of Health and Human Service regulations and standards.

Cell Culture

The 4T1 mouse mammary carcinoma cell line was obtained from American Type Culture Collection (Rockville, MD). B16F10-sTAC melanoma cells engineered to express SIINFEKL peptide were kindly provided by Dr. Adam Snook (Thomas Jefferson University, Philadelphia, PA). B16F10-sTAC and 4T1 cells were cultured in DMEM supplemented with 10% fetal bovine serum and 1x Penicillin/Streptomycin (Cellgro). The cells were freshly thawed from early passage cells and cultured for no more than 2 months. Cell line authentication by chromosomal analysis and short tandem repeat (STR)-based DNA profiling as well as IMPACT tests to verify the absence of murine pathogens and mycoplasma (IDEXX BioAnalytics, Columbus, MO) were performed on these cells before use in animal experiments.

Drugs

Working solutions of the ODC inhibitor DFMO (kindly donated by Dr. Patrick Woster at the University of South Carolina) were prepared in sterile water. The Trimer PTI (Figure 1A) was synthesized as previously described [10], and 1 mM stock solutions were prepared in sterile PBS and stored at −20°C. Chemical authentication of the Trimer PTI included ^{1}H NMR, ^{13}C NMR, mass spectrometry, melting point, and elemental analysis of the final compound used in this study.

Bone marrow derived myeloid cells

For macrophage cultures, bone marrow was flushed from the femurs C57BL/6 or *Odc*$^{\Delta Mye}$ mice with RPMI under sterile conditions, red blood cells lysed in lysis buffer (0.17 M Tris-HCL, 0.16 M NH_4Cl) for 3 minutes, and then resuspended in bone marrow media (RPMI, 10% heat inactivated FBS and 1% penicillin/streptomycin). Cells were plated in 100 mM uncoated Petri dishes with 10 ml of bone marrow media containing 20 ng/ml macrophage colony stimulating factor (M-CSF) (R&D Systems, 216MC025). On day two, an additional 10 ml of bone marrow media containing 20 ng/ml M-CSF was added. On day five, 10 ml of media was gently removed and 10 mL of bone marrow media containing 20 ng/ml M-CSF was added. By day 7, adherent cells had differentiated into macrophages. Macrophages were polarized to M1 or M2 with 100 ng/ml LPS (Sigma, L2630) or 10 ng/ml IL-4 (R&D Systems, 404-ML-010), respectively.

MDSC were generated from bone marrow precursor cells by flushing bone marrow aseptically from femurs of C57Bl/6 mice [18]. Red blood cells were lysed with lysis buffer, and the remaining cells were cultured for 4 days at 5×10^5 cells per well in 6-well dishes in bone marrow media supplemented with 60 ng/ml GM-CSF and 60 ng/ml IL-6 (ProSpec, CYT-222 and CYT-213). Before harvest of nonadherent MDSCs and adherent monocytes at 4 days, some cells were treated with bone marrow media containing PBT (final concentrations: 0.25 mM DFMO and 1 μM Trimer PTI) for 24 h, 48 h or 96 h.

Arginase/iNOS assays

Differentiated but unpolarized bone marrow derived macrophages were plated in 96-well dishes at 5×10^5 cells per well and cultured for 24 h in bone marrow media supplemented with LPS (100 ng/ml), IL-4 (10 ng/ml), or tumor conditioned media (4T1 tumor cells cultured in bone marrow media for 48 hours and then filtered to remove cell debris). To test for M1 polarization, nitric oxide generation was measured via a Greiss assay (Sigma, G4410). An arginase assay was performed as an endpoint for M2 polarization. Briefly, cells were lysed in a 100 μl solution of 0.1% Triton X-100 + Halt protease/phosphatase cocktail (Fisher Scientific, PI78441) with shaking for 30 minutes, followed by addition of 100 μl of 50 mM Tris-HCl to each well. 100 μl of cell lysate was removed and placed into Eppendorf tubes, 10 μl of 10 mM $MnCl_2$ was added, and the samples were incubated at 55°C for 10 minutes. Once heated, 100 μl of 0.5 M L-arginine was added to each sample and incubated for 1 hour at 37°C. The reaction was stopped by the addition of 800 μl of stop buffer ($7H_2O$:$3H_2PO_4$:$1H_2SO_4$) and 40 μl of 9% isonitrosopropiophenone in ethanol. The lysates were heated at 100°C for 45 minutes, absorbance read at 540 nm, and then normalized to protein levels in the lysates.

Zymography and Immunoblotting

Bone marrow derived macrophages were grown to 80% confluency, polarized with IL-4 overnight, then washed twice with PBS and refed with serum-free RPMI. After 48 h the conditioned media was collected and centrifuged at 600 × g to remove cell debris. Samples were separated on a 10% zymography gel containing 0.1% gelatin (Novex, ZY00100BOX). MMP-2 and MMP-9 activity was detected by incubating the gel in 1x zymography renaturing buffer (Novex, LC2670) for 30 min at room temperature followed by 1x developing buffer (Novex, LC2671) for 24 h at 37°C. After Coomassie staining, the bands of proteolytic degradation were quantified.

For immunoblots, adherent and non-adherent MDSC cells were lysed in RIPA buffer (Thermo Fisher Scientific, 89900) containing Halt protease/phosphatase cocktail (Fisher Scientific, PI78441). Proteins were separated by SDS-polyacrylamide gel (Invitrogen, Hercules, CA), transferred to polyvinylidene difluoride (PVDF) membranes (Millipore, Temecula, CA), and briefly stained with Ponceau S (Sigma, St. Louis, MO) to verify efficient transfer. Immunoblots were blocked with 5% non-fat dry milk followed by an overnight incubation at 4°C with a rabbit polyclonal antibody against p-STAT3 (Y705) (Cell Signaling, Danvers, MA) followed by a secondary antibody conjugated to horseradish peroxidase. Antibody binding was detected by chemiluminescence (ECL Plus Western Blotting Detection System, Amersham/GE Healthcare, Piscataway, NJ). Membranes were re-probed with a mouse monoclonal antibody against β-actin (Sigma, St. Louis, MO) to verify equal loading of protein.

In Vivo tumor models

Tumor models were established by subcutaneous injections of 5×10^5 B16F10-sTAC melanoma cells in C57Bl6 mice or by orthotopic injection of 2×10^4 4T1 cells in the mammary fat pad of Balb/c mice. Before treatments were initiated, mice were randomized into groups with similar mean tumor volumes and standard deviations. Treatment with 0.25% (w/v) DFMO in the drinking water and Trimer PTI (3 mg/kg daily by intraperitoneal [i.p.] injection) was initiated when tumors were palpable (50–100 mm^3). In experiments with anti-PD-1 monoclonal antibody (mAb) or anti-Ly6G mAb, 100 μg of anti-PD-1 mAb (clone RMP1–14, BioXCell), anti-Ly6G mAb (clone RB6–8C5, BioXCell), or isotype control (rat IgG2a mAb, clone 2A3, BioXCell) were administered i.p. every other day for three total doses starting one week before treatment with DFMO and Trimer PTI was initiated. Tumor growth was assessed morphometrically using calipers twice a week, and tumor volumes were calculated using the formula $V\ (mm^3) = \pi/6 \times A \times B^2$ (A is the larger diameter and B is the smaller diameter) [19].

Flow cytometry analysis of immune cells

Tumor tissue was digested in a 0.3% collagenase/0.1% hyaluronidase solution, pressed through a nylon mesh filter to obtain a single cell suspension, incubated in red cell lysis buffer for 3 minutes, and the cell pellet resuspended in FACS buffer (PBS + 1.5% FBS). Equal numbers of viable cells were stained with a viability dye and combinations of the following antibodies: CD8a-PECy7, CD4-PE, F4/80-PECy7,CD206-FITC, Ly6G-APC, Ly6C-PerCP-Cy5.5, CD11b-PE, CD45-PE-Cy5, IFN-γ-APC, CD80-APC, CD11c-FITC,

PD-L1-PE, and SIINFEKL pentamer-PE. For Cyto-ID staining, cells were first stained for surface markers (Gr1 and CD11b or F4/80 and CD206) followed by staining with Cyto-ID for 30 min at 37°C, per the manufacturer's protocol (Enzo Life Sciences, ENZ-51031). Flow cytometric data were acquired on a BD FACSCanto II cytometer and analyzed using FACSDiva software (BD Biosciences).

Antigen-specific T-cell response detection by IFN-γ ELISpot

Upon sacrifice, splenocytes from B16F10-sTAC tumor-bearing mice were analyzed for IFN-γ producing cells by enzyme-linked immunosorbent spot (ELISpot) assay. Multiscreen filtration plates (Millipore, MSHAN4550) were coated with 0.5 μg/ml of purified anti-mouse IFN-γ capture antibody (BioLegend) overnight at 4˚C. Single-cell suspensions of splenocytes or tumors were plated at 1×10^6 per well. Splenocytes were stimulated with the SIINFEKL peptide (Anaspec, AS-60193–1) at 20 μg/ml. After 16 hours of stimulation at 37˚C, the cells were removed by washing and spots were developed with a biotinylated anti-IFN-γ detection antibody (BioLegend) and streptavidin-horseradish peroxidase conjugate followed by NITRO-blue tetrazolium chloride and 5-bromo-4-chloro-3'-indoylphosphate p-toluidine salt substrate (Sigma, B5655–25TAB). Spot numbers were counted, and data were reported as IFN-γ-spot forming cells per 10^6 cells.

Statistical analysis

All *in vitro* experiments were performed at least in triplicate, and data were compiled from two to three separate experiments. Analyses were done using a 1-way ANOVA with a Tukey test for statistical significance or a Students t-test. *In vivo* studies were carried out using multiple animals (n = 5–10 per treatment group based on previous repeated murine tumor experiments). The mean profile plots were created in Stata/MP 15.1 (StataCorp LP., Texas, USA) and all other analyses were performed in SAS 9.4 SAS/STAT Version 14.1 for Windows (SAS Institute Inc., Cary, NC, USA). All tests were two-sided and the statistical significance level was set to 0.05. Since tumor volume grew exponentially over time, all volumes were transformed and analyzed on the logarithmic (base 10) scale. All means and standard errors presented were back-transformed to represent geometric means and standard errors [20]. Since tumor volume was measured longitudinally for each mouse, linear mixed-effects models were used to evaluate change in tumor volume over time. In the models, log tumor volume was the response and time, treatment, and the interaction between time and treatment were the fixed effects, and mouse was considered a random effect. The Kaplan-Meier estimator was used to estimate the survival functions, and the log-rank test was used to compare two or more survival distributions. To control the type I error, p-values were corrected using the Holm-Bonferroni method for any analysis which compared > 2 groups.

Results

PBT therapy reduces tumor growth and metastasis

To evaluate the anti-tumor effect of polyamine blockade therapy (PBT), we used the 4T1 metastatic breast cancer model. After orthotopic injection of 4T1 cells into the mammary fat pad of syngeneic Balb/c mice, treatment was initiated three weeks post injection. Mice were administered Trimer PTI (3 mg/kg, i.p., daily) and 0.25% DFMO (w/v) in the drinking water

(Figure 1A) [9, 10]. Treatment with Trimer PTI and DFMO significantly inhibited growth of the primary tumor, resulting in a three-fold reduction in the final tumor volume in PBT treated mice compared to control untreated mice (Figure 1A). Moreover, treatment with PBT resulted in a six-fold reduction in metastatic nodules in the lungs of 4T1 tumor bearing mice compared to untreated control mice and (Figure 1B).

The 4T1 tumor model is characterized by a large influx and accumulation of immature $Gr1^+CD11b^+$ MDSCs that contribute to immune suppression by blocking $CD4^+$ and $CD8^+$ T cell activation [21, 22]. MDSCs in mice can be either monocytic ($Ly6C^+CD11b^+$) or granulocytic ($Ly6G^+CD11b^+$) with the predominant species in the 4T1 tumors being $Ly6G^+/CD11b^+$ granulocytic MDSCs (Figures 1C and 1D). Interestingly, co-treatment with Trimer PTI and DFMO resulted in large reductions in both $Ly6G^+CD11b^+$ granulocytic MDSCs and pro-tumorigenic $F480^+/CD206^+$ M2-like macrophages (Figure 1E) in the tumors of 4T1-tumor bearing mice compared to vehicle treated mice, but had no effect on the levels of $Ly6C^+CD11b^+$ monocytic MDSCs (Figure 1D). Because of the dramatic reduction in $Ly6G^+CD11b^+$ granulocytic MDSCs observed with PBT therapy, we treated 4T1 tumor-bearing mice with anti-Ly6G antibody before initiation of PBT therapy to investigate what effect depletion of granulocytic MDSCs would have on PBT anti-tumor efficacy. Treatment with anti-Ly6G antibody reduced tumor growth in control vehicle-treated mice but demonstrated no additional anti-tumor effects in mice treated with PBT (Figure 1E), suggesting that PBT may be directly targeting these pro-tumorigenic $Ly6G^+$ myeloid cells.

Recent studies have identified cytoprotective autophagy as a key molecular pathway involved in promoting the survival of MDSCs [22, 23]. We hypothesized that changes in polyamine metabolism may modify autophagy levels in tumor-infiltrating, immunosuppressive myeloid cell subpopulations to facilitate their survival and pro-tumorigenic activity. To examine this, we used a flow cytometry-based assay with the fluorescent dye Cyto-ID that colocalizes with LC3 on autophagosomes to assess the effect of PBT treatment on levels of autophagic flux in leukocytes in the tumor, lung metastases and the spleen. As expected, the percentage of $CD45^+$ leukocytes was lower in 4T1 tumors compared to that in lungs and spleens of tumor-bearing mice (Figure 2A). Overall, macrophages and MDSCs comprised more than 95% of the total leukocytes in all three tissue types (Supplemental Figure 1). Treatment with PBT reduced levels of tumor-infiltrating leukocytes compared to levels in control tumors but had no impact on leukocyte levels in the spleen or in lungs with metastatic lesions. To directly compare leukocyte subpopulations in different treatment groups in tumors, lung, and spleen, all cell numbers were normalized to their respective control group. The overall numbers of autophagic leukocytes were highest in tumors of 4T1 tumor bearing mice and were significantly reduced by PBT therapy (Figure 2B). Interestingly, PBT had no effect on autophagy levels in the lung metastases or spleen indicating that autophagy may be more important in the microenvironment of the tumor than in the spleen or lung. Evaluation of the tumor-infiltrating leukocyte subpopulations isolated from 4T1 tumors revealed that PBT-reductions in levels of leukocyte autophagy were due primarily to reduced autophagy in $Gr1^+CD11b^+$ MDSCs and pro-tumorigenic $F480^+/CD206^+$ M2-like macrophages but not in $CD4^+$ or $CD8^+$ T-cells (Figures 2C–F). Because 4T1 tumors have very low levels of cytotoxic $CD8^+$ T-cells compared to the number of immunosuppressive MDSCs and M2 macrophages

(Supplemental Figure 1), reducing cytoprotective autophagy in myeloid cells and their resulting decrease in number may allow the immune system to mount a stronger anti-tumor response.

Polyamine metabolism is vital for M2-like polarization of macrophages and MDSC differentiation

Due to the reduction in M2-like macrophages in the tumors of PBT treated mice, we hypothesized that polyamine metabolism is an important factor in M2 polarization of macrophages. To investigate this further, we used bone marrow-derived macrophages from either C57Bl/6 mice or $Odc^{\Delta Mye}$ mice that have a myeloid cell-specific deletion of ODC [16], the rate-limiting enzyme in polyamine biosynthesis. Monocytes were isolated from bone marrow, differentiated into macrophages with M-CSF, and then treated with LPS to promote M1 polarization or with either IL-4 or tumor cell-conditioned media to promote M2 polarization. Using arginase activity as a measure of the M2 phenotype, we observed that $Odc^{\Delta Mye}$ macrophages were weakly induced to an M2 phenotype by IL-4 or tumor cell-conditioned media compared to wildtype C57Bl/6 macrophages (Figure 3A). Conversely, $Odc^{\Delta Mye}$ macrophages displayed a more robust M1 phenotype when polarized with LPS as measured by iNOS activity compared to WT B6 macrophages (Figure 3B). As would be expected given their lack of ODC, $Odc^{\Delta Mye}$ macrophages displayed higher basal levels of polyamine transport activity compared to wildtype C57Bl/6 macrophages (Figure 3C). M1 polarization did not affect the rates of polyamine transport activity in either wildtype C57Bl/6 or $Odc^{\Delta Mye}$ macrophages but M2 polarization led to a 2-fold increase in polyamine transport in wildtype C57Bl/6 macrophages, demonstrating the increased need for polyamines during M2 polarization (Figure 3C). Incubation of $Odc^{\Delta Mye}$ macrophages with IL-4 resulted in only a small increase in polyamine transport, indicating that the polyamine transport system may be operating at near maximal levels at baseline and unable to increase transport in response to signals for M2 polarization. To test whether PBT blocks IL-4 induced M2 polarization of macrophages, wildtype C57Bl/6 macrophages were treated with either Trimer PTI, DFMO or Trimer PTI plus DFMO during polarization with IL-4. M2 polarization, measured by arginase activity, was inhibited by PBT combination therapy, but not by Trimer PTI or DFMO alone indicating that restrictions to polyamine biosynthesis and polyamine transport are required to inhibit M2 polarization of macrophages (Figure 3D).

Bone marrow derived macrophages polarized with IL-4 or tumor conditioned media also displayed less surface markers of M2-polarization when treated with PBT, demonstrated by dramatically reduced levels of CD206 (Figure 4A) and PD-L1 (Figure 4B) compared to untreated cells. Analysis of supernatants collect from M2 and unpolarized control macrophages revealed that M2 macrophages polarized with IL-4 secreted higher levels of matrix metalloproteinase-2 and −9 (MMP-2 and MMP-9), which has been associated with higher levels of tumor cell invasion and metastasis, compared to unpolarized macrophages (Figure 4C). Treatment with DFMO significantly reduced MMP-2 and MMP-9 secretion from M2 macrophages while co-treatment with both Trimer-PTI and DFMO reduced secretion of both MMP-2 and MMP-9 from M2 macrophages to levels lower than was observed in control macrophages.

Given the dramatic reduction of MDSCs *in vivo* in 4T1 tumor bearing mice treated with PBT, we hypothesized that PBT may be impacting MDSC differentiation. To examine this, we examined the effect of PBT on MDSC cultures differentiated from bone marrow precursor cells Four day cultures of both nonadherent and adherent cells were predominantly $Ly6G^+CD11b^+$; however, nearly half of the adherent cells expressed the F480 macrophage marker (Supplemental Figure 2). When MDSC cultures were treated with PBT (0.25 mM DFMO + 1 μM Trimer PTI), there was a stepwise increase in the percentage of $F480^+/CD80^+$ and $F480^+/CD11c^+$ cells over time in the macrophage adherent population but not in the nonadherent population of $Ly6G^+CD11b^+$ MDSCs (Figure 5A, 5B). The PBT induction of the M1 macrophage markers CD80 and CD11c [24] suggested that PBT can redirect the differentiation of MDSCs to pro-inflammatory M1-like macrophages. In line with this observation, PBT treatment of MDSC cultures also down-regulated expression of p-STAT3, an oncogenic transcription factor whose activation is implicated in MDSC differentiation and survival [25], in non-adherent cells but not the adherent cells (Figure 5C).

PBT and PD-1 blockade work synergistically to inhibit tumor growth and increase survival

Because PBT reduces levels of the immunosuppressive MDSCs and M2 macrophages in the tumor microenvironment, we hypothesized that PBT will have synergistic anti-tumor activity with PD-1 blockade, which relieves suppression of cytotoxic T-cell activity by blocking PD-L1/PD-1 signaling. 4T1 tumor bearing mice were treated with three doses of anti-PD-1 mAb or isotype control mAb beginning one week before PBT therapy was initiated. Mice receiving anti-PD-1 mAb alone saw no reduction in tumor growth compared to control mice (Figure 6). PBT therapy significantly reduced the rate of tumor growth compared to control mice, but the combination therapy of both PBT and anti-PD-1 mAb was the most efficacious resulting in a 4-fold reduction in final tumor volume compared to control and anti PD-1 mAb alone and a 50% reduction compared to PBT therapy alone.

To confirm the results observed in the 4T1 breast cancer model, co-treatment with PBT and anti-PD-1 mAb was then tested in mice injected with B16F10-sTAC melanoma cells that express the SIINFEKL peptide. As was observed in the 4T1 tumor model, the combination therapy of PBT and anti-PD-1 mAb was significantly more effective than PBT or anti-PD-1 mAb alone (Figure 7A). The decrease in tumor growth in B16F10-sTAC tumor-bearing mice treated with PBT was associated with a significant increase in the number of IFN-γ producing splenocytes as measured by an ELISpot assay following *ex vivo* stimulation with the SIINFEKL peptide (Figure 7B). Treatment with the anti-PD-1 mAb increased IFN-γ spot formation, but not significantly. Co-treatment with PBT and anti-PD-1 mAb significantly increased IFN-γ spot formation compared to that with either PBT or anti-PD-1 mAb alone. Pentamer analysis of the SIINFEKL recognition site on $CD8^+$ cytotoxic T-cells revealed that only mice co-treated with PBT and anti-PD-1 mAb had substantially higher frequencies of SIINFEKL-specific $CD8^+$ T cells compared to that seen in B16F10 tumor-bearing control mice (Figure 7B). A survival study showed that co-treatment with PBT and anti-PD-1 mAb decreased tumor growth (Supplemental Figure 3) and significantly increased the survival of B16F10 tumor-bearing mice (Figure 7D).

Overall these data suggest that PBT significantly inhibits tumor growth in multiple tumor models by reducing cytoprotective autophagy in MDSCs and M2 macrophages and alleviating the immunosuppressive tumor microenvironment. Furthermore, these data show that PBT in combination with anti-PD-1 mAb synergistically inhibits tumor growth and increases survival.

Discussion

Tumors require elevated levels of polyamines for not only providing biomass via increased protein translation, enhanced survival, and metastasis of the epithelial tumor cells, but also by modulating the generation, survival, and activity of tumor-infiltrating immune cell subpopulations. In this study we show that PBT-mediated polyamine blockade in tumors decreases cytoprotective autophagy in tumor-infiltrating MDSCs and macrophages, thus contributing to decreased tumor growth and metastasis. Along with the dramatic PBT-induced decrease in major immunosuppressive myeloid cells in the tumor, PBT also significantly increases tumor-specific cytotoxic T-cells, enhances the anti-tumor efficacy of PD-1 blockade, and increases the survival of tumor-bearing animals. We show in two different tumor models that tumor growth is significantly inhibited in tumor-bearing mice co-treated with anti-PD-1 mAb and PBT compared to anti-PD-1 mAb alone or PBT alone.

MDSCs and M2-like TAMs are characterized by high levels of arginase 1. Indeed, arginine metabolism plays a central role in the function of immune cells. Immunosuppressive tumor-infiltrating myeloid cells can promote tumor progression by degrading arginine in the tumor microenvironment and depriving T cells what is an essential amino acid for T cell activation and function [11]. Polyamine biosynthesis is dependent on the activity of arginase to supply ornithine as a substrate for ODC. With this intersection of arginine and polyamine metabolism, elevated polyamine biosynthesis in both tumor epithelial cells and infiltrating MDSCs and TAMs contribute to a depletion of extracellular arginine leading to T-cell dysfunction. Polyamine production also appears to regulate macrophage polarization in that polyamines restrain M1 activation and promote M2 alternative activation [13, 14]. Hardbower et al. showed that *H. pylori* and *C. rodentium* infection in $Odc^{\Delta Mye}$ transgenic mice increases gastritis and colitis, respectively, and enhances production of M1 proinflammatory cytokines of macrophages [16, 17]. However, they reported that bone marrow-derived macrophages from $Odc^{\Delta Mye}$ transgenic mice still showed enhanced expression of M2 markers following stimulation with IL-4 [16]. Our data show that decreasing polyamine biosynthesis with DFMO inhibition of ODC activity, a myeloid-specific deletion of *ODC* in $Odc^{\Delta Mye}$ mice, or blocking polyamine uptake with the Trimer PTI alone did not inhibit IL-4 induction of arginase to the same extent as treatment with both DFMO and the Trimer PTI, suggesting that both polyamine biosynthesis and increased polyamine uptake are needed to increase intracellular polyamine levels to contribute to the M2-polarization of macrophages. Spermidine can also be enzymatically converted to hypusine that post-translationally modifies and activates the translation factor eIF5A [26]. Recently Puleston et al. [27] showed that polyamine-dependent hypusinated eIF5A induces mitochondrial oxidative phosphorylation that promotes M2 polarization in macrophages [27]. In addition, spermidine production by MDSCs has been shown to induce an indoleamine 2,3-dioxygenase 1 (IDO1)-dependent, immunosuppressive phenotype in

tolerogenic dendritic cells [28]. Because PBT depletion of polyamines inhibits STAT3 activation that drives MDSC formation while reprogramming bone marrow progenitor cells to differentiate to M1-like macrophages, we speculate that polyamines are also important regulators of MDSC generation. Thus, PBT activates an anti-tumor immune response via multiple mechanisms that affect the metabolism of not only tumor epithelial cells and cytotoxic T cells but also immunosuppressive tumor-associated cell populations.

In addition to effects of polyamines on macrophage polarization and function, polyamines can contribute to macrophage survival via induction of autophagy [29]. Autophagy is a common adaptive resistance mechanism when tumor cells face metabolic or therapeutic stress [30]. Autophagy has also been shown to regulate the differentiation of macrophages into pro-tumorigenic TAMs [31, 32], and it plays a role in the suppressive role and survival of tumor MDSCs [23, 33, 34]. Autophagy in these immunosuppressive myeloid cells can be induced by cellular stressors such as nutrient and growth factor deprivation and hypoxia, all characteristics of a malignant tumor microenvironment [35–37]. One mechanism by which tumor immunosuppressive MDSCs survive their harsh tumor microenvironment is to assume a cytoprotective autophagic state [18, 38]. Polyamines can also induce an autophagic state, thus contributing to tumor survival [39–42]. For instance, spermidine has been shown to induce autophagy in yeast cells, *C. elegans*, Drosophila, and human tumor cells [41, 43] and to increase survival of pluripotent stem cells in culture [44]. In addition, our results suggest that increased polyamine biosynthesis and uptake may contribute to an autophagic state in tumor immunosuppressive myeloid subpopulations such as MDSCs and TAMs. We show that the autophagic flux in tumor-infiltrating M2-like macrophages and MDSCs is significantly decreased following treatment with both DFMO and Trimer PTI. Importantly, autophagic flux was most elevated in tumor-infiltrating MDSC and TAM populations and significantly decreased with PBT treatment only in these myeloid cell subpopulations in tumors. These results suggest that the anti-tumor activity of PBT is due, at least in part, to its selective elimination of tumor-infiltrating immunosuppressive myeloid populations.

Whereas PBT appears to inhibit pro-tumorigenic M2 polarization of macrophages, there are many examples demonstrating a heterogeneous macrophage population in tumors resulting from rapidly changing stimuli in this complex *in vivo* microenvironment [45]. Metabolic rewiring in tumor epithelial cells affects other cell types, including tumor-infiltrating immune cells, via nutrient competition and metabolites that act as signaling molecules [46–49]. Since polyamine levels are important in all cell types, it is likely that lowering polyamine levels in the tumor microenvironment not only affects macrophage and MDSC populations but also modulates the function of various tumor T cell populations, such as tissue resident memory T cells whose activation can contribute to the increased tumor-specific cytotoxic T cell response following PBT [50]. Moreover, elevated polyamine metabolism in tumor cells impacts not only arginine but also methionine metabolism, and changes in cellular polyamine levels affect the activity of chromatin-modifying enzymes that control both histone methylation and acetylation [16, 51]. Specific to M1 polarization, ODC-depleted macrophages demonstrate changes in histone methylation marks including increased histone 3, lysine 4 (H3K4) mono-methylation and H3K9 acetylation but decreased H3K9 di/trimethylation that have been associated with open chromatin leading to increased transcription [16]. Thus, polyamine-modulated epigenetic enzymes most likely play a role in

activation of immune cell types and the immunosuppressive activity of TAMs and MDSCs by altering gene expression leading to metabolic reprogramming.

Tumors evade immune surveillance via a variety of different mechanisms including the activation of immune checkpoint pathways such as the PD-1/PD-L1 pathway that suppress an anti-tumor immune response. However, MDSCs and immunosuppressive TAMs are major obstacles to immune checkpoint blockade anti-tumor efficacy. We show that PBT treatment decreases these tumor-infiltrating immunosuppressive myeloid populations and increases tumor-specific cytotoxic T cell populations. Our results highlight the powerful activity of PBT treatment in reinvigorating the T-cell directed activity of immune checkpoint blockade and promoting immune-mediated elimination of tumor cells. Since ICB is only effective in a subset of cancer patients, our results suggest that PBT may improve the therapeutic anti-tumor and anti-metastatic efficacy of ICB in currently resistant patients.

Supplementary Material

Refer to Web version on PubMed Central for supplementary material.

Acknowledgements

This work was supported by research grants to S.G. from the Dept. of Defense, National Institutes of Health, the John B. Deaver Foundation, and Biostrategy Partners.

Abbreviations

DFMO	α-difluoromethylornithine
H3K4	histone 3, lysine 4
IDO1	indoleamine 2,3-dioxygenase
IL-4	interleukin 4
ICB	immune checkpoint blockade
LPS	lipopolysaccharide
M-CSF	macrophage colony-stimulating factor
MMP-2 and MMP-9	metalloprotease-2 and −9
MDSCs	myeloid derived suppressor cells
NOS	nitric oxidase synthase
ODC	ornithine decarboxylase
PBT	polyamine blocking therapy
PTI	polyamine transport inhibitor
PD-L1	programmed cell death ligand-1

PD-1	programmed cell death protein-1
TAMs	tumor associated macrophages

References

1. Adams S, Schmid P, Rugo HS, Winer EP, Loirat D, Awada A, Cescon DW, Iwata H, Campone M, Nanda R et al.: Pembrolizumab Monotherapy for Previously Treated Metastatic Triple-Negative Breast Cancer: Cohort A of the Phase 2 KEYNOTE-086 Study. Ann Oncol 2018.
2. Adams S, Loi S, Toppmeyer D, Cescon DW, De Laurentiis M, Nanda R, Winer EP, Mukai H, Tamura K, Armstrong A et al.: Title: Pembrolizumab Monotherapy for Previously Untreated, PD-L1-Positive, Metastatic Triple-Negative Breast Cancer: Cohort B of the Phase 2 KEYNOTE-086 Study. Ann Oncol 2018.
3. Gerner EW, Meyskens FL, Jr. : Polyamines and cancer: old molecules, new understanding. Nat Rev Cancer 2004, 4(10):781–792. [PubMed: 15510159]
4. Casero RA, Jr., Murray Stewart T, Pegg AE: Polyamine metabolism and cancer: treatments, challenges and opportunities. Nat Rev Cancer 2018, 18(11):681–695. [PubMed: 30181570]
5. Bello-Fernandez C, Packham G, Cleveland JL: The ornithine decarboxylase gene is a transcriptional target of c-Myc. Proc Natl Acad Sci USA 1993, 90:7804–7808. [PubMed: 8356088]
6. Origanti S, Shantz LM: Ras transformation of RIE-1 cells activates cap-independent translation of ornithine decarboxylase: regulation by the Raf/MEK/ERK and phosphatidylinositol 3-kinase pathways. Cancer Res 2007, 67(10):4834–4842. [PubMed: 17510413]
7. Chang BK, Libby PR, Bergeron RJ, Porter CW: Modulation of polyamine biosynthesis and transport by oncogene transfection. Biochem Biophys Res Commun 1988, 157(1):264–270. [PubMed: 3143363]
8. Peters MC, Minton A, Phanstiel Iv O, Gilmour SK: A Novel Polyamine-Targeted Therapy for BRAF Mutant Melanoma Tumors. Med Sci (Basel) 2018, 6(1).
9. Alexander ET, Minton A, Peters MC, Phanstiel Ot, Gilmour SK: A novel polyamine blockade therapy activates an anti-tumor immune response. Oncotarget 2017, 8(48):84140–84152. [PubMed: 29137411]
10. Muth A, Madan M, Archer JJ, Ocampo N, Rodriguez L, Phanstiel Ot: Polyamine transport inhibitors: design, synthesis, and combination therapies with difluoromethylornithine. J Med Chem 2014, 57(2):348–363. [PubMed: 24405276]
11. Rodriguez PC, Quiceno DG, Zabaleta J, Ortiz B, Zea AH, Piazuelo MB, Delgado A, Correa P, Brayer J, Sotomayor EM et al.: Arginase I production in the tumor microenvironment by mature myeloid cells inhibits T-cell receptor expression and antigen-specific T-cell responses. Cancer Res 2004, 64(16):5839–5849. [PubMed: 15313928]
12. Sinha P, Clements VK, Ostrand-Rosenberg S: Reduction of myeloid-derived suppressor cells and induction of M1 macrophages facilitate the rejection of established metastatic disease. J Immunol 2005, 174(2):636–645. [PubMed: 15634881]
13. Van den Bossche J, Lamers WH, Koehler ES, Geuns JM, Alhonen L, Uimari A, Pirnes-Karhu S, Van Overmeire E, Morias Y, Brys L et al.: Pivotal Advance: Arginase-1-independent polyamine production stimulates the expression of IL-4-induced alternatively activated macrophage markers while inhibiting LPS-induced expression of inflammatory genes. J Leukoc Biol 2012, 91(5):685–699. [PubMed: 22416259]
14. Zhang M, Caragine T, Wang H, Cohen PS, Botchkina G, Soda K, Bianchi M, Ulrich P, Cerami A, Sherry B et al.: Spermine inhibits proinflammatory cytokine synthesis in human mononuclear cells: a counterregulatory mechanism that restrains the immune response. J Exp Med 1997, 185(10):1759–1768. [PubMed: 9151701]
15. Latour YL, Gobert AP, Wilson KT: The role of polyamines in the regulation of macrophage polarization and function. Amino Acids 2019.
16. Hardbower DM, Asim M, Luis PB, Singh K, Barry DP, Yang C, Steeves MA, Cleveland JL, Schneider C, Piazuelo MB et al.: Ornithine decarboxylase regulates M1 macrophage activation and

mucosal inflammation via histone modifications. Proceedings of the National Academy of Sciences of the United States of America 2017, 114(5):E751–e760. [PubMed: 28096401]

17. Singh K, Coburn LA, Asim M, Barry DP, Allaman MM, Shi C, Washington MK, Luis PB, Schneider C, Delgado AG et al.: Ornithine Decarboxylase in Macrophages Exacerbates Colitis and Promotes Colitis-Associated Colon Carcinogenesis by Impairing M1 Immune Responses. Cancer Res 2018, 78(15):4303–4315. [PubMed: 29853605]
18. Parker KH, Sinha P, Horn LA, Clements VK, Yang H, Li J, Tracey KJ, Ostrand-Rosenberg S: HMGB1 Enhances Immune Suppression by Facilitating the Differentiation and Suppressive Activity of Myeloid-Derived Suppressor Cells. Cancer Res 2014, 74(20):5723–5733. [PubMed: 25164013]
19. Buzzai M, Jones RG, Amaravadi RK, Lum JJ, DeBerardinis RJ, Zhao F, Viollet B, Thompson CB: Systemic treatment with the antidiabetic drug metformin selectively impairs p53-deficient tumor cell growth. Cancer Res 2007, 67(14):6745–6752. [PubMed: 17638885]
20. Shaw RMS, Curwen J, Dymond M: Design, analysis and reporting of tumor models. Lab Animal 2017, 46(5):207–211. [PubMed: 28422097]
21. Pulaski BA, Ostrand-Rosenberg S: Mouse 4T1 breast tumor model. Curr Protoc Immunol 2001, Chapter 20:Unit 20 22.
22. Ostrand-Rosenberg S, Beury DW, Parker KH, Horn LA: Survival of the fittest: how myeloid-derived suppressor cells survive in the inhospitable tumor microenvironment. Cancer Immunol Immunother 2019.
23. Parker KH, Horn LA, Ostrand-Rosenberg S: High-mobility group box protein 1 promotes the survival of myeloid-derived suppressor cells by inducing autophagy. J Leukoc Biol 2016, 100(3):463–470. [PubMed: 26864266]
24. Zhu Y, Zhang L, Lu Q, Gao Y, Cai Y, Sui A, Su T, Shen X, Xie B: Identification of different macrophage subpopulations with distinct activities in a mouse model of oxygen-induced retinopathy. Int J Mol Med 2017, 40(2):281–292. [PubMed: 28627621]
25. Yu H, Kortylewski M, Pardoll D: Crosstalk between cancer and immune cells: role of STAT3 in the tumour microenvironment. Nature reviews Immunology 2007, 7(1):41–51.
26. Park MH, Nishimura K, Zanelli CF, Valentini SR: Functional significance of eIF5A and its hypusine modification in eukaryotes. Amino Acids 2010, 38(2):491–500. [PubMed: 19997760]
27. Puleston DJ, Buck MD, Klein Geltink RI, Kyle RL, Caputa G, O'Sullivan D, Cameron AM, Castoldi A, Musa Y, Kabat AM et al.: Polyamines and eIF5A Hypusination Modulate Mitochondrial Respiration and Macrophage Activation. Cell metabolism 2019, 30(2):352–363. [PubMed: 31130465]
28. Mondanelli G, Bianchi R, Pallotta MT, Orabona C, Albini E, Iacono A, Belladonna ML, Vacca C, Fallarino F, Macchiarulo A et al.: A Relay Pathway between Arginine and Tryptophan Metabolism Confers Immunosuppressive Properties on Dendritic Cells. Immunity 2017, 46(2):233–244. [PubMed: 28214225]
29. Zhou S, Gu J, Liu R, Wei S, Wang Q, Shen H, Dai Y, Zhou H, Zhang F, Lu L: Spermine Alleviates Acute Liver Injury by Inhibiting Liver-Resident Macrophage Pro-Inflammatory Response Through ATG5-Dependent Autophagy. Front Immunol 2018, 9:948. [PubMed: 29770139]
30. Mowers EE, Sharifi MN, Macleod KF: Functions of autophagy in the tumor microenvironment and cancer metastasis. Febs j 2018, 285(10):1751–1766. [PubMed: 29356327]
31. Zhang Y, Morgan MJ, Chen K, Choksi S, Liu ZG: Induction of autophagy is essential for monocyte-macrophage differentiation. Blood 2012, 119(12):2895–2905. [PubMed: 22223827]
32. Ngabire D, Kim GD: Autophagy and Inflammatory Response in the Tumor Microenvironment. Int J Mol Sci 2017, 18(9).
33. Fletcher M, Ramirez ME, Sierra RA, Raber P, Thevenot P, Al-Khami AA, Sanchez-Pino D, Hernandez C, Wyczechowska DD, Ochoa AC et al.: l-Arginine depletion blunts antitumor T-cell responses by inducing myeloid-derived suppressor cells. Cancer Res 2015, 75(2):275–283. [PubMed: 25406192]
34. Alissafi T, Hatzioannou A, Mintzas K, Barouni RM, Banos A, Sormendi S, Polyzos A, Xilouri M, Wielockx B, Gogas H et al.: Autophagy orchestrates the regulatory program of tumor-associated myeloid-derived suppressor cells. J Clin Invest 2018, 128(9):3840–3852. [PubMed: 29920188]

35. Kroemer G, Marino G, Levine B: Autophagy and the integrated stress response. Mol Cell 2010, 40(2):280–293. [PubMed: 20965422]
36. Schaaf MB, Cojocari D, Keulers TG, Jutten B, Starmans MH, de Jong MC, Begg AC, Savelkouls KG, Bussink J, Vooijs M et al.: The autophagy associated gene, ULK1, promotes tolerance to chronic and acute hypoxia. Radiother Oncol 2013, 108(3):529–534. [PubMed: 23849170]
37. Corzo CA, Condamine T, Lu L, Cotter MJ, Youn JI, Cheng P, Cho HI, Celis E, Quiceno DG, Padhya T et al.: HIF-1alpha regulates function and differentiation of myeloid-derived suppressor cells in the tumor microenvironment. J Exp Med 2010, 207(11):2439–2453. [PubMed: 20876310]
38. Parker KH, Horn LA, Ostrand-Rosenberg S: High-mobility group box protein 1 promotes the survival of myeloid-derived suppressor cells by inducing autophagy. J Leukoc Biol 2016, 100(3):463–470. [PubMed: 26864266]
39. Cufi S, Vazquez-Martin A, Oliveras-Ferraros C, Martin-Castillo B, Vellon L, Menendez JA: Autophagy positively regulates the CD44 (+) CD24 (-/low) breast cancer stem-like phenotype. Cell Cycle 2011, 10(22):3871–3885. [PubMed: 22127234]
40. Mirzoeva OK, Hann B, Hom YK, Debnath J, Aftab D, Shokat K, Korn WM: Autophagy suppression promotes apoptotic cell death in response to inhibition of the PI3K-mTOR pathway in pancreatic adenocarcinoma. J Mol Med 2011, 89(9):877–889. [PubMed: 21678117]
41. Morselli E, Marino G, Bennetzen MV, Eisenberg T, Megalou E, Schroeder S, Cabrera S, Benit P, Rustin P, Criollo A et al.: Spermidine and resveratrol induce autophagy by distinct pathways converging on the acetylproteome. The Journal of cell biology 2011, 192(4):615–629. [PubMed: 21339330]
42. Morselli E, Galluzzi L, Kepp O, Marino G, Michaud M, Vitale I, Maiuri MC, Kroemer G: Oncosuppressive functions of autophagy. Antioxid Redox Signal 2011, 14(11):2251–2269. [PubMed: 20712403]
43. Eisenberg T, Knauer H, Schauer A, Buttner S, Ruckenstuhl C, Carmona-Gutierrez D, Ring J, Schroeder S, Magnes C, Antonacci L et al.: Induction of autophagy by spermidine promotes longevity. Nature cell biology 2009, 11(11):1305–1314. [PubMed: 19801973]
44. Chen T, Shen L, Yu J, Wan H, Guo A, Chen J, Long Y, Zhao J, Pei G: Rapamycin and other longevity-promoting compounds enhance the generation of mouse induced pluripotent stem cells. Aging Cell 2011, 10(5):908–911. [PubMed: 21615676]
45. Van den Bossche J, O'Neill LA, Menon D: Macrophage Immunometabolism: Where Are We (Going)? Trends Immunol 2017, 38(6):395–406. [PubMed: 28396078]
46. Colegio OR: Lactic acid polarizes macrophages to a tumor-promoting state. Oncoimmunology 2016, 5(3):e1014774. [PubMed: 27141329]
47. Corrado M, Scorrano L, Campello S: Changing perspective on oncometabolites: from metabolic signature of cancer to tumorigenic and immunosuppressive agents. Oncotarget 2016, 7(29):46692–46706. [PubMed: 27083002]
48. Bunse L, Pusch S, Bunse T, Sahm F, Sanghvi K, Friedrich M, Alansary D, Sonner JK, Green E, Deumelandt K et al.: Suppression of antitumor T cell immunity by the oncometabolite (R)-2-hydroxyglutarate. Nat Med 2018, 24(8):1192–1203. [PubMed: 29988124]
49. Van den Bossche J, Saraber DL: Metabolic regulation of macrophages in tissues. Cell Immunol 2018, 330:54–59. [PubMed: 29395037]
50. Park SL, Gebhardt T, Mackay LK: Tissue-Resident Memory T Cells in Cancer Immunosurveillance. Trends Immunol 2019, 40(8):735–747. [PubMed: 31255505]
51. Hobbs CA, Gilmour SK: High levels of intracellular polyamines promote histone acetyltransferase activity resulting in chromatin hyperacetylation. J Cell Biochem 2000, 77(3):345–360. [PubMed: 10760944]

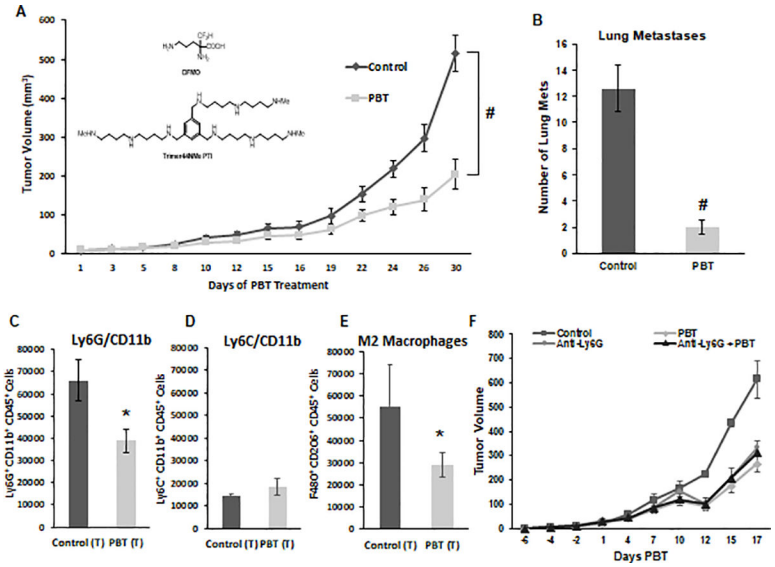

Figure 1. Inhibition of 4T1 tumor growth and metastasis with DFMO and Trimer PTI.

A. Mice were orthotopically injected in the mammary fat pad with 2×10^4 4T1 mammary carcinoma cells. Three weeks following injection of 4T1 cells when tumors were approximately 40 mm^3 in size, treatment was initiated with either control vehicle or PBT (0.25% DFMO (w/v) in the drinking water plus Trimer PTI [3 mg/kg, i.p., once a day]). Graph shows 4T1 tumor growth under different treatments (mean tumor volume ± SEM). Inset shows the structures of DFMO and the Trimer PTI. **B.** Lung metastasis were counted following perfusion of lungs with India Ink upon sacrifice (mean ± SEM). Upon sacrifice, tumors were excised from 4T1-tumor bearing mice and equal numbers of cells were analyzed by flow cytometry. Infiltrating $CD45^+$ leukocytes analyzed for (**C**) granulocytic MDSCs ($Ly6G^+/CD11b^+$) ± SEM, (**D**) monocytic MDSCs ($Ly6C^+/CD11b^+$) ± SEM and (**E**) M2 macrophages ($F4/80^+/CD206^+$) ± SEM. (**F**) Mice were orthotopically injected in the mammary fat pad with 2 × 104 4T1 mammary carcinoma cells. Two weeks later mice were injected with 100 ug of anti-Ly6G mAb or isotype control antibody (i.p., three total doses administered every other day). Three weeks following 4T1 cell injections, treatment was initiated with either saline or PBT as described in earlier, and tumor growth was measured. n = 10 mice per group; * = $p \leq 0.05$ and # = $p \leq 0.01$ compared to vehicle treated mice.

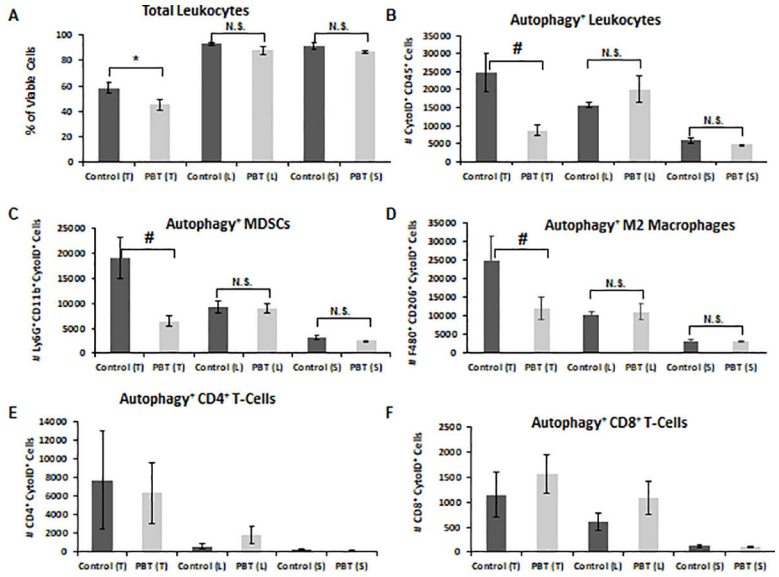

Figure 2. DFMO and Trimer PTI reduced autophagy in immunosuppressive leukocytes.

Mice were orthotopically injected in the mammary fat pad with 2×10^4 4T1 mammary carcinoma cells. Three weeks following injection of 4T1 cells, treatment was initiated with either control vehicle or PBT. Mice were sacrificed after three weeks of treatment, and equal numbers of cells from tumors (T), lungs (L), and spleens (S) were analyzed by flow cytometry for, **A**: total leukocytes ($CD45^+$), **B**: autophagic activity in $CD45^+$ leukocytes ($CytoID^+CD45^+$), **C**: autophagy$^+$ MDSCs ($CytoID^+Gr1^+CD11b+$), **D**: autophagy$^+$ M2 macrophages ($CytoID^+F480^+CD206^+$), **E**; autophagy$^+$ $CD4^+$ T-cells ($CytoID^+CD4^+$), **F**: autophagy$^+$ $CD8^+$ T-cells ($CytoID^+CD8^+$). n = 10 per group ± SEM; * = $p \leq 0.05$ and # = $p \leq 0.01$ compared to vehicle treated mice.

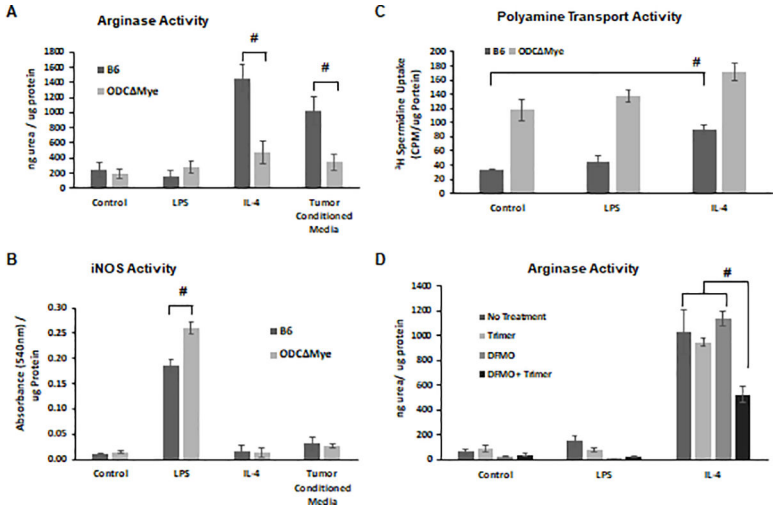

Figure 3. Polyamines promote polarization to a M2 phenotype in macrophages.

Primary bone marrow-derived monocytes were isolated from wildtype C57Bl/6 and *Odc*$^{\Delta Mye}$ transgenic mice. *Odc*$^{\Delta Mye}$ mice have a myeloid cell-specific deletion of the polyamine biosynthetic enzyme ODC. Bone marrow derived monocytes were differentiated to macrophages with M-CSF and then polarized to an M1 phenotype with LPS or to a M2 phenotype with either IL-4 or tumor cell-conditioned media. (**A**) Arginase activity (ng urea produced/μg protein ± SD) was used to assess the M2 phenotype of macrophages while (**B**) iNOS activity (absorbance at 540 nm ± SD) was used to quantify the M1 phenotype. (**C**) Polyamine transport activity (^{3}H-spermidine uptake/ μg protein ± SD) was measured via an ^{3}H-spermidine uptake assay. (**D**) The ability of DFMO ± Trimer PTI to inhibit M2 polarization of bone marrow derived macrophages was assessed via an arginase activity assay (ng urea produced/μg protein ± SD). n = 8; * = $p \leq 0.05$ and # = $p \leq 0.01$ compared to control.

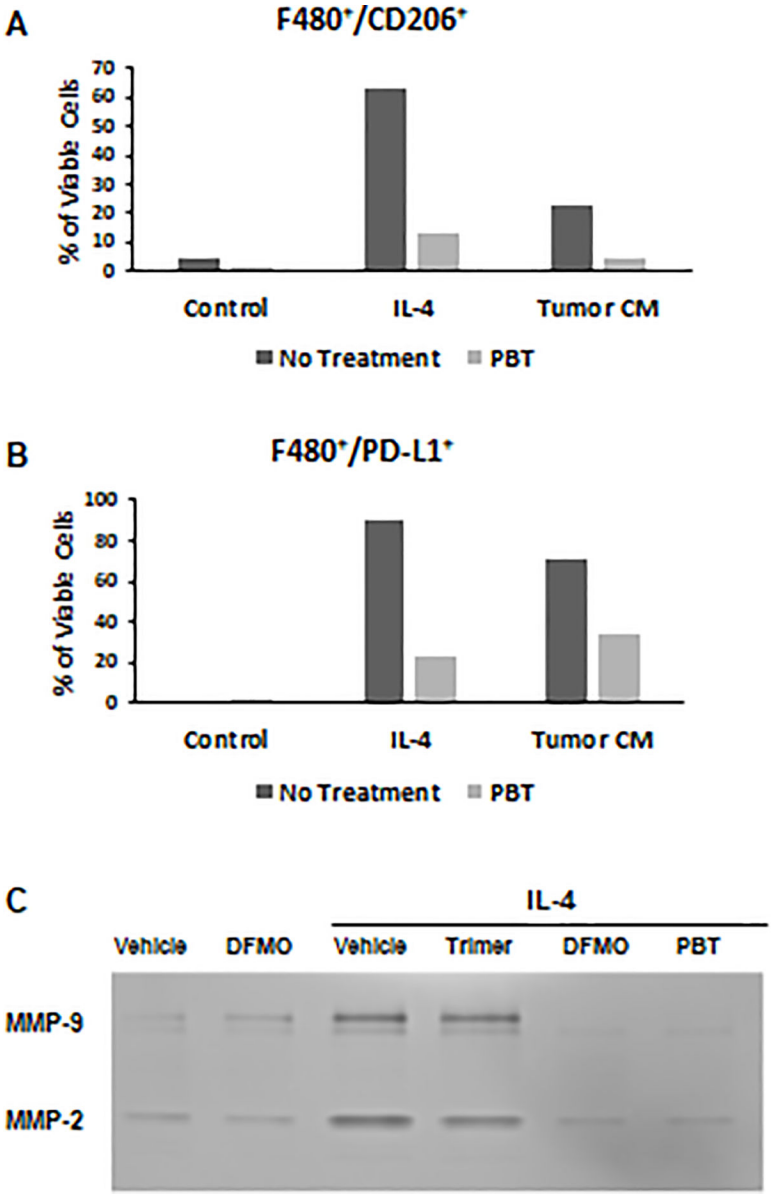

Figure 4. PBT inhibits pro-tumorigenic properties of M2 macrophages.

Bone marrow derived macrophages were treated for 16 h with IL-4 (10 ng/ml) ± 1.0 μM Trimer PTI and 0.25 mM DFMO and were analyzed by flow cytometry for surface expression of (**A**) $F480^{+}CD206^{+}$ and (**B**) $F480^{+}PD\text{-}L1^{+}$ markers. (**C**) Conditioned media was collected from treated macrophages and subjected to zymography analysis of MMP-2 and MMP-9 activity. Results are representative of three separate experiments.

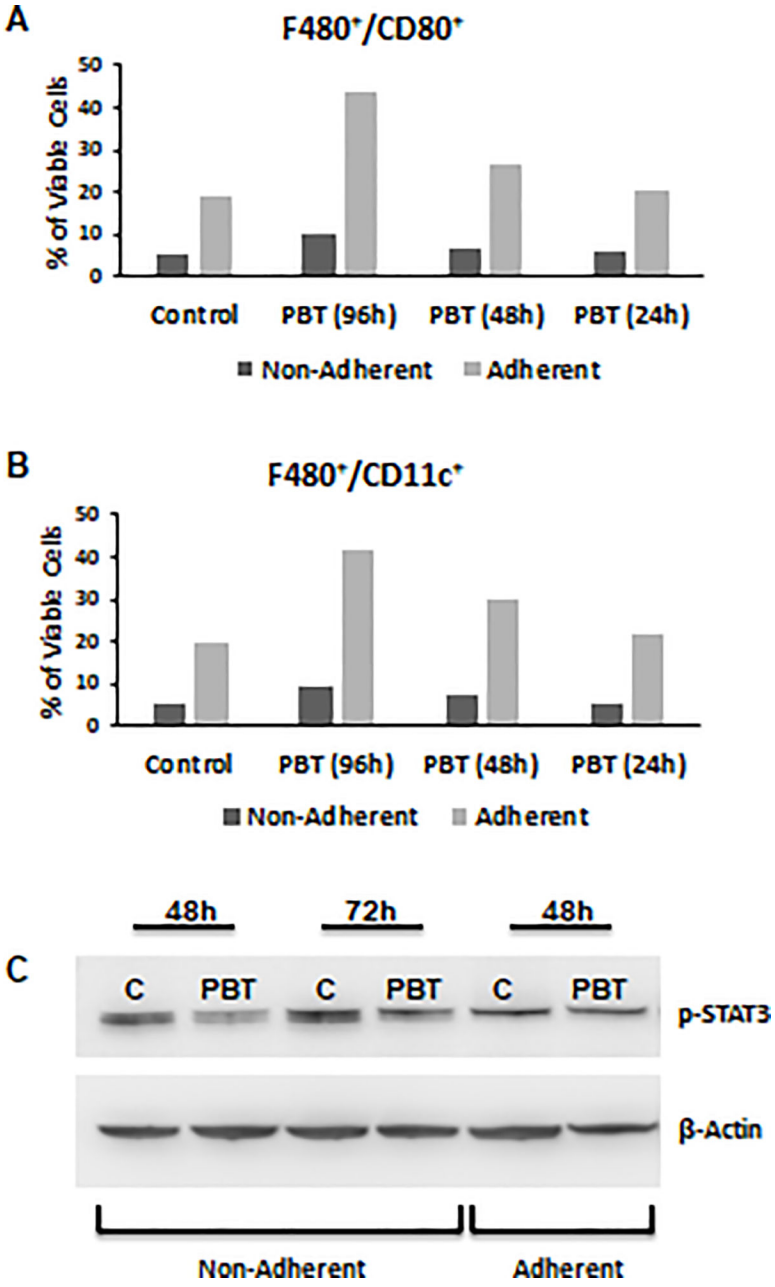

Figure 5. PBT promotes conversion of immature MDSCs to M1 macrophages.

Bone marrow precursor cells were cultured with GM-CSF (60 ng/ml) and IL-6 (60 ng/ml) for 96 h. MDSC cultures were treated with PBT (0.25 mM DFMO and 1 uM Trimer) concurrent with GM-CSF and IL-6 for the last 24 h, 48 h or the entire 96 h in culture. Adherent and non-adherent cells were analyzed by flow cytometry for expression of (**A**) $F480^{+}CD80^{+}$ and (**B**) $F480^{+}CD11c^{+}$ markers. (**C**) Four-day cultures of MDSCs were treated ± PBT for 48 or 72 h. Cell lysates were prepared from both adherent and non-adherent cells and analyzed by immunoblot assay for p-STAT3 levels and probed for β-actin as a loading control. Representative of three separate experiments.

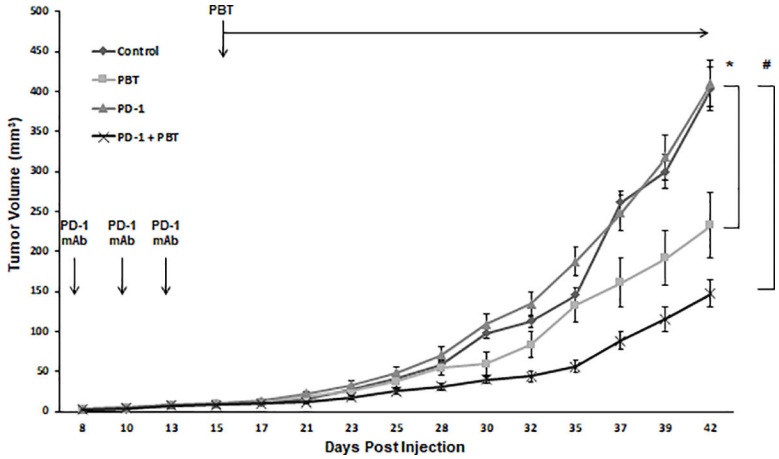

Figure 6. 4T1 tumor growth inhibition with PBT plus anti-PD-1 blockade.

Mice were orthotopically injected in the mammary fat pad with 2×10^4 4T1 mammary carcinoma cells. Doses of 100 μg anti-PD-1 mAb or 100 μg isotype control mAb were administered on days 8, 11 and 14. On day 16, treatment was initiated with either saline or PBT (0.25% DFMO (w/v) in the drinking water plus Trimer PTI [3 mg/kg, i.p., daily]). Graph shows 4T1 tumor growth with different treatments (mean tumor volume ± SEM). n = 10 mice per group; * = $p \leq 0.05$ and # = $p \leq 0.01$ compared to vehicle treated mice.

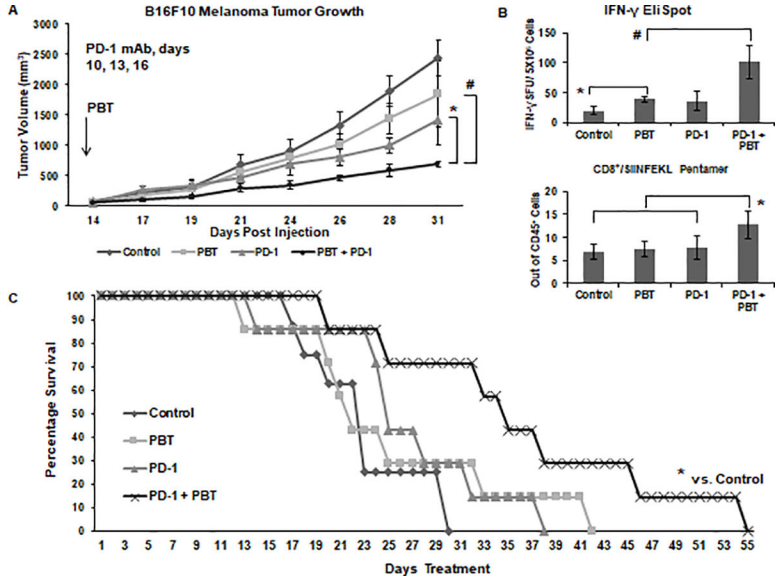

Figure 7. B16F10-sTAC tumor growth inhibition with PBT plus anti-PD-1 blockade.

(**A**) Mice were subcutaneously injected with 5×10^5 B16F10-sTAC melanoma cells expressing SIINFEKL. Doses of 100 μg anti-PD-1 mAb or isotype control mAb were administered on days 10, 13 and 16. On day 14, treatment was initiated with either saline or PBT (0.25% DFMO (w/v) in the drinking water plus Trimer PTI [3 mg/kg, i.p., daily]). Graph shows B16F10-sTAC tumor growth with different treatments (mean tumor volume ± SEM). (**B**) Top panel: The frequency of IFN-γ producing T-cells following challenge with SIINFEKL peptide was measured by the ELISpot assay as IFN-γ spot forming units (SFU) per million spleen cells ± SEM. Bottom panel: The percentage of $CD8^+$/SIINFEKL $Pentamer^+$ infiltrating leukocytes ± SEM from the tumors of B16F10-sTAC tumor-bearing mice in different treatment groups. (**C**) Survival of B16F10-sTAC tumor-bearing mice with different treatment regimens. n = 7–10 mice per group; * = $p \leq 0.05$ and # = $p \leq 0.01$ compared to vehicle treated mice.